FEBS 29351 FEBS Letters 579 (2005) 1619–1624

Comparative single-turnover kinetic analyses of *trans*-cleaving hammerhead ribozymes with naturally derived non-conserved sequence motifs

Marc S. Weinberg, John J. Rossi*

Division of Molecular Biology, Beckman Research Institute of the City of Hope, Graduate School of Biological Sciences, Duarte, CA 91010, USA

Received 3 January 2005; revised 31 January 2005; accepted 1 February 2005

Available online 18 February 2005

Edited by Hans-Dieter Klenk

Abstract ***trans*-Cleaving hammerhead ribozyme variants were generated with mimicked non-conserved internal loop motifs derived from five structurally diverse natural *cis*-cleaving ribozymes. Most modified *trans*-cleaving variants showed enhanced single-turnover cleavage rates relative to minimal counterparts that lack tertiary interactions between internal loop motifs I and II, and relative to controls with sequence changes in loop I. The *trans*-cleaving ribozyme derived from the positive strand of peach latent mosaic viroid had the highest observed cleavage rate, suggesting a structurally optimized motif that facilitates rapid formation of the ribozyme catalytic center in a *trans*-reaction.**

Keywords: Hammerhead ribozyme; HIV-1

1. Introduction

The hammerhead ribozyme was first identified as a self-cleaving motif in strands of both polarity within viroid and viroid-like satellite RNA sequences [1,2] and later discovered within repetitive satellite DNA sequences of caudate amphibians, *Dolichopoda* cave cricket species and schistosomes [3–5].

The hammerhead ribozyme catalytic core, which consists of 15 highly conserved nucleotides at the junction of three helices, was determined in early boundary experiments by removing nucleotides originally thought to be non-essential [6,7]. However, a recent re-examination of the kinetics of natural self-cleaving (*cis*-cleaving) hammerhead ribozymes, which each have distinct helical-loop motifs not associated with the catalytic core, shows much higher cleavage rates than was originally determined [8,9]. *cis*-Hammerhead ribozymes possess tertiary "kissing loop" interactions between loops I and II or between loop II and an internal bulge in helix I that significantly affect the cleavage rate [8–10]. Moreover, enhanced cleavage of an endogenous complementary substrate has been achieved in *trans* for a hammerhead ribozyme derived from *Schistosoma mansoni*, Smα1, [11,12]. Cleavage is efficient even at submillimolar concentrations of Mg^{2+}, where tertiary interactions between peripheral loop motifs allow for folding of the hammerhead ribozyme in a structurally active conformation, thus diminishing the need for higher Mg^{2+} ion concentrations required for active folding of the minimal *trans*-cleaving ribozyme [11,13].

In this study, *trans*-cleaving hammerhead ribozyme variants were made with alterations in the hybridizing arm of helix I aimed at comparing tertiary interactions found in natural *cis*-cleaving hammerhead ribozymes with structurally different peripheral sequences. We show that most modified *trans*-cleaving ribozymes targeted to the same exogenous substrate have enhanced single-turnover *trans*-activities relative to minimal derivatives, with the most catalytically effective motifs those that likely adopt an already optimized natural tertiary stabilizing structure.

2. Materials and methods

2.1. Hammerhead ribozyme template and substrate sequences

Double-stranded DNA fragments encoding hammerhead ribozymes were assembled by annealing two synthetic oligonucleotides (Integrated DNA Technologies) with 18 nucleotides of partial sequence complementarity followed by two cycles of PCR. The cDNAs were cloned into the TA vector pCR2.1 (Invitrogen) followed by sequencing. To generate templates for transcription, ribozyme-encoding plasmid DNAs were substrates for a second PCR using a forward primer containing the T7 promoter sequence (underlined) as a 5′-linker (5′-GATCATTGTAATACGACTCACTATAGGG-3′) and a reverse primer specific to 18 bases of the 3′ ribozyme sequence. To assess the differences in cleavage rate between modified *trans*-cleaving hammerhead ribozymes and controls using manual quenching methods without changing the reaction conditions (by altering $[Mg^{2+}]$ or pH), a 5′ CUC 3′ cleavage triplet (underlined) was chosen as opposed to the more efficiently cleaved canonical 5′ GUC 3′ [14]. The 5′ GUC 3′ triplet is cleaved with an observed first-order rate constant (k_{obs}) of approximately 1 min^{-1} for a kinetically well-behaved minimal hammerhead ribozyme under "standard" conditions of 50 mM Tris–Cl, pH 7.5, 25 °C, 10 mM $MgCl_2$ [15]. The substrate RNA 5′-UGUGCCUCUUCAGCUACC-3′ (found in the replication-competent HIV-1 vector pNL4-3, Genbank Accession No. AF324439) was chemically synthesized at the City of Hope DNA, RNA and Peptide Synthesis Facility.

2.2. In vitro transcription reaction

To generate *trans*-acting hammerhead ribozyme RNA, transcription was performed using Ambion's Megashortscript kit according to the manufacturer's instructions at 37 °C for 3 h in a 20 μl final volume. Following treatment with 2 U DNase I (Promega), RNA was extracted with chloroform–phenol and precipitated with ethanol. Substrate RNA was 5′ labeled with [γ-^{32}P]ATP (7000 Ci/mmol; MP Biomedicals) and T4 polynucleotide kinase as previously described in [16].

*Corresponding author. Fax: +1 626 301 8271.
E-mail address: Jrossi@coh.org (J.J. Rossi).

0014-5793/$30.00
doi:10.1016/j.febslet.2005.02.016

2.3. trans-*Cleavage single-turnover kinetics*

trans-Cleavage rate kinetics was investigated under single-turnover conditions [15]. Ribozymes (720 nM) and labeled substrate (7 nM) were first annealed by heating to 95 °C for 2 min followed by cooling to 37 °C for 10 min in 50 mM Tris–HCl at pH 7.0, and 100 mM NaCl. Aliquots were removed at specific time intervals following the addition of $MgCl_2$ (to a final concentration of 1 or 10 mM). Reactions were quenched with 2 volumes of 95% (v/v) formamide containing 50 mM EDTA, 0.2% bromophenol blue and 0.2% xylene cyanol. Fragments were resolved by 15% (w/v) denaturing (7 M Urea) PAGE. Quantitative values were determined by phosphorimager analysis using a Typhoon 9410 Variable Mode Imager (Amersham Biosciences) and ImageQuant 5.2. (Molecular Dynamics). In order to determine the observed first-order rate constant (k_{obs}), the data were fit to either a single- or double-exponential association [15].

3. Results

3.1. *Single-turnover cleavage kinetics for* trans-*cleaving hammerhead ribozyme variants of sTRSV(+)*

Initially, the natural hammerhead ribozyme derived from satellite RNA of tobacco ringspot virus, sTRSV(+) (Fig. 1A) was chosen since its sequence is used for most standard minimal *trans*-cleaving ribozyme constructs. Two modified *trans*-cleaving versions, sTRSV-L1 and sTRSV- L1 var2, were generated where the sTRSV(+) loop I sequence was placed in the hybridizing arm of helix I (Fig. 1A) such that the resulting loop/bulge and catalytic core are six nucleotides apart and closely resemble the wild-type structure. At 10 mM Mg^{2+}, a ~4-fold improvement in k_{obs} (0.43 min^{-1}) was observed for sTRSV-L1 when compared to the minimal *trans*-cleaving ribozyme, sTRSV-min (0.10 min^{-1}) (Fig. 1B and Table 1). Moreover, sTRSV-L1 sustained its enhanced activity at 1 mM Mg^{2+}, where the difference was ~9-fold versus sTRSV-min. In contrast, sTRSV-L1 var2, which has a GCC clamp anchoring loop I, was largely ineffective (k_{obs} = 0.02 min^{-1}) even though this structure theoretically preserves the natural shape of loop I. Variant sTRSV-L1 var2 likely adopts a catalytically inactive conformation. To determine whether the difference in cleavage rate is affected by the sequence composition of loop I, wild-type loop I sequences in sTRSV-L1 were replaced by a CUCUCUC loop in the variant sTRSV-L1* CU resulting in a ~2-fold reduction in cleavage rate when compared to sTRSV-L1. The reaction for sTRSV-L1* CU was bi-phasic, indicating the formation of an alternative inactive

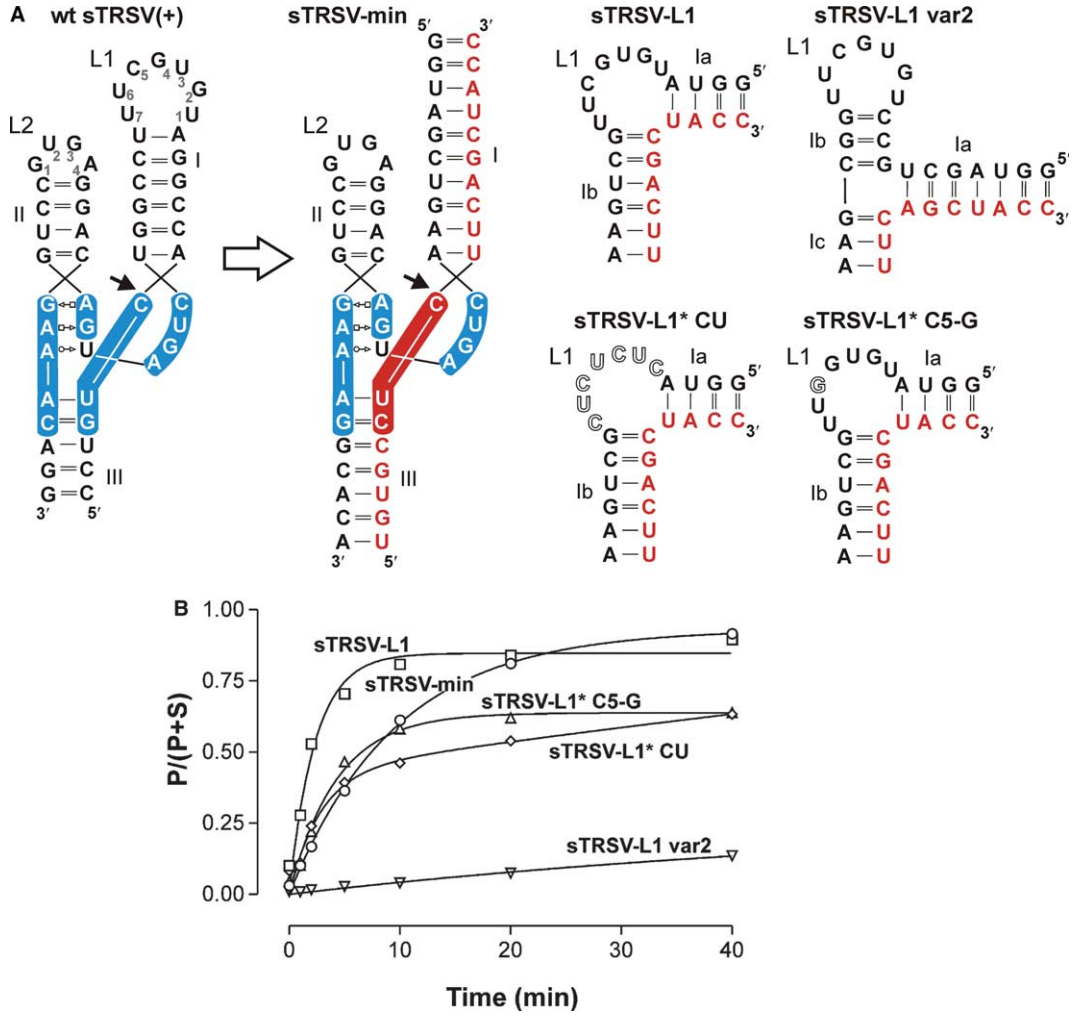

Fig. 1. Secondary structure diagrams and cleavage time-course for *trans*-cleaving variants of sTRSV(+). (A) A two-dimensional schematic representation of *cis*- and *trans*-cleaving hammerhead ribozymes. Catalytic core nucleotides for in *cis* (blue) and in *trans* (red) cleavage are shaded. The substrate sequence is in red. Where possible, canonical and non-canonical base-pair interactions are shown in the classification of Leontis and Westhof [22]. A closed arrow indicates the cleavage site. Loop I nucleotides that differ from natural sequences are outlined. (B) Time-course of *trans*-cleavage at 10 mM $MgCl_2$ for sTRSV(+) variants: sTRSV-L1 (square), sTRSV-min (circle), sTRSV-L1* C5-G (triangle), sTRSV-L1* CU (diamond) and sTRSV-L1 var2 (inverted triangle). Fraction cleaved, P/(P + S), is shown as a function of time (min). Kinetic parameters are summarized in Table 1.

Table 1
Kinetic parameters for *trans*-cleaving hammerhead ribozymes

Ribozyme	k_{obs} (min^{-1})[a]	Change in activity (fold)[b]	F_∞[c]
sTRSV-min	0.10 (<0.01)	1	0.93
sTRSV-L1	0.43 (0.09)	4.3	0.87
sTRSV-L1 var2	0.02	5	0.27
sTRSV-L1* CU	0.22	2.2	0.63
sTRSV-L1* C5-G	0.23	2.3	0.58
PLMVd-min	0.04	1	0.53
PLMVd-L1	0.82 (0.26)	21	0.93
PLMVd-L1* A3-C	0.07	1.75	0.66
CChMVd-min	<0.01	1	0.06
CChMVd-L1	0.29	>29	0.54
CChMVd-L1* CU	0.04	>4	0.43
Smα1-L1	0.14	n.d	0.95
Smα1-L1 Δ1a	0.02	n.d	0.88
Pst3-L1	n.m	n.d	n.m

n.m., not measurable; n.d., not determined; the values for k_{obs} and F_∞ represent the mean of two independent measurements.
[a]Measurements were made at 37 °C in 50 mM Tris–HCl, pH 7.0, 100 mM NaCl and 10 mM $MgCl_2$. k_{obs} values determined using 1 mM $MgCl_2$ are shown in parentheses.
[b]Change in activity is the k_{obs} from the *trans*-cleaving ribozyme variants of sTRSV(+), PLMVd(−) and CChMVd(+) at 10 mM $MgCl_2$ divided by each respective minimal *trans*-cleaving hammerhead ribozyme.
[c]F_∞ is the fraction cleaved at the end-point of the reaction.

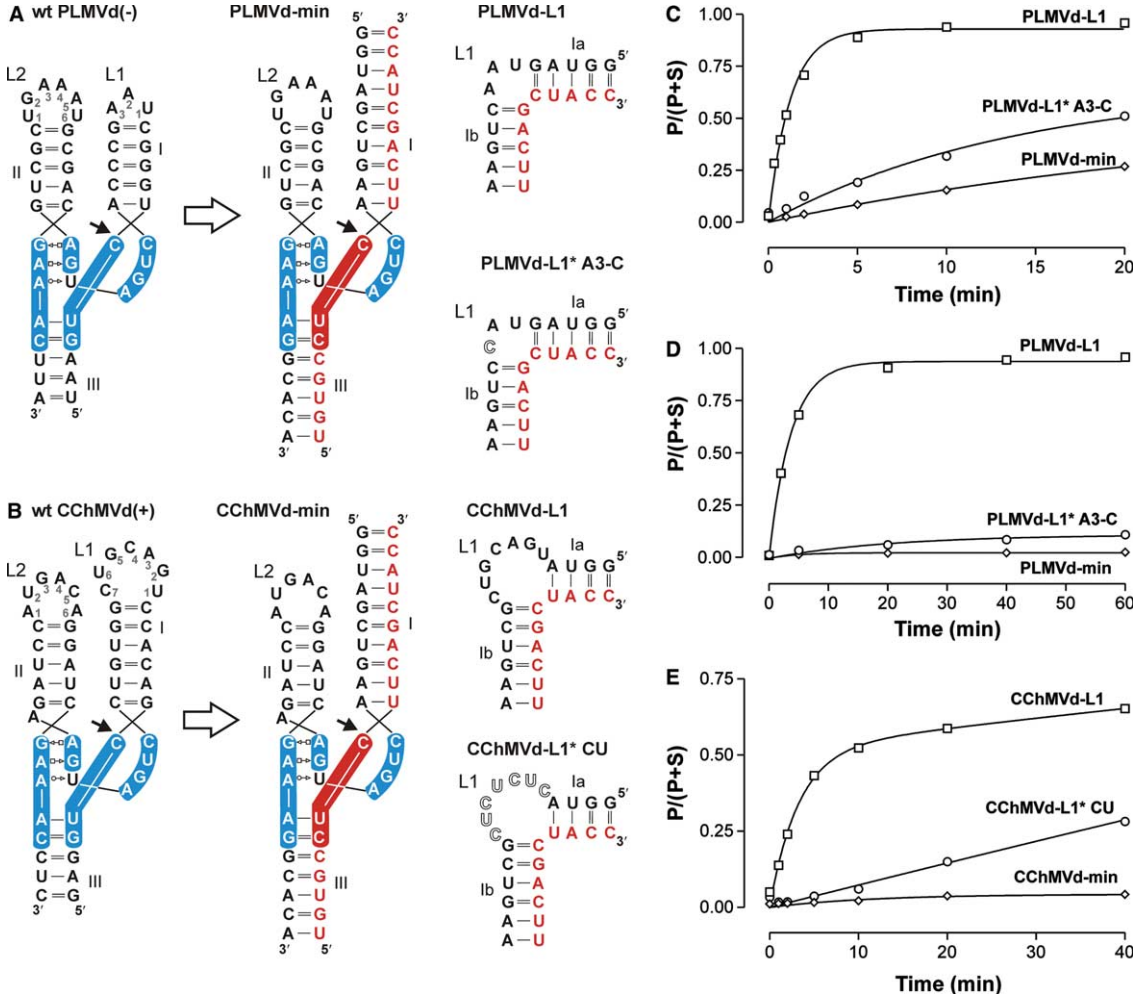

Fig. 2. Secondary structure diagrams and cleavage time-course for *trans*-cleaving variants of (A) PLMVd(−) and (B) CChMVd(+). (C) Time-course of *trans*-cleavage at 10 mM $MgCl_2$ for PLMVd(−) variants: PLMVd-L1 (square), PLMVd-min (diamond) and PLMVd-L1* A3-C (circle). (D) Time-course of *trans*-cleavage for PLMVd(−) variants (labeled as for C) at 1 mM $MgCl_2$. (E) Time-course of *trans*-cleavage 10 mM $MgCl_2$ for CChMVd(+) variants: CChMVd-L1 (square), CChMVd-min (diamond) and CChMVd-L1* CU (circle). Figure annotations are described in Fig. 1. Kinetic parameters are summarized in Table 1.

enzyme–substrate complex that is in slow exchange with the active conformation (Fig. 1B). When guanosine was replaced with cytosine at position 5 in loop I, enhanced *cis*-cleavage was observed [8]. However, the equivalent replacement in sTRSV-L1* C5-G yielded a reduced cleavage rate relative to sTRSV-L1 (Fig. 1B and Table 1), suggesting that the structural features adopted by the modified ribozyme variants are only partially analogous to their *cis*-cleaving counterparts.

3.2. *Single-turnover cleavage kinetics for* trans*-cleaving hammerhead ribozyme variants of PLMVd(−) and CChMVd(+)*

Natural hammerhead ribozyme loops I and II differ significantly in their size, sequence composition and distance from the catalytic core [17]. To investigate the effect of structurally diverse loop–loop interactions in a *trans*-ribozyme context, helical-loop motifs derived from the negative strand of peach latent mosaic viroid (PLMVd) [18] and the positive strand of chrysanthemum chlorotic mottled viroid (CChMVd) [19] were adapted similarly to sTRSV(+). Variant PLMVd-L1, with a 5′ UAA 3′ bulge inserted into helix I (Fig. 2A), showed a 21-fold increase in k_{obs} relative to its minimal control, PLMVd-min (Fig. 2C and Table 1), and a ~17-fold increase relative to PLMVd-L1* A3-C (Fig. 2C and Table 1), which has a cytosine replacing adenosine at position 3 in loop I (Fig. 2A). Even at 1 mM $MgCl_2$, PLMVd-L1 cleaved more efficiently than the standard minimal *trans*-cleaving variant sTRSV-min at 10 mM $MgCl_2$ (2-fold increase in k_{obs}). The difference in cleavage rate was even greater when compared to both PLMVd-min and PLMVd-L1* A3-C, which were largely ineffective at 1 mM $MgCl_2$ (Fig. 2D) suggesting that PLMVd-L1 retains its activity at low Mg^{2+} ion concentrations.

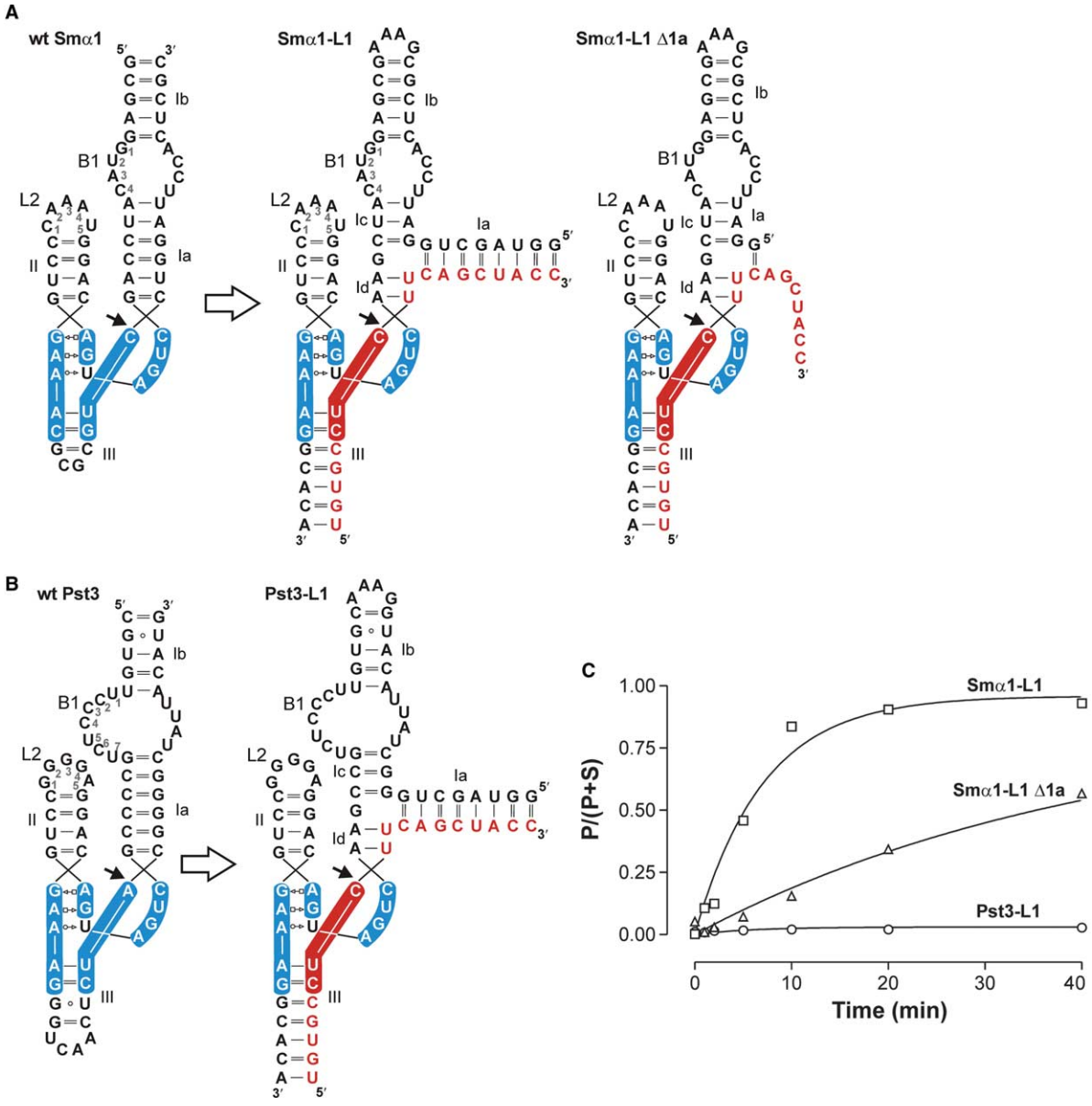

Fig. 3. Secondary structure diagrams and cleavage time-course for *trans*-cleaving variants of Smα1 and Pst3. (A) A two-dimentional schematic representation of *cis*- and *trans*-cleaving hammerhead ribozyme sequences is shown. (B) Time-course at 10 mM $MgCl_2$ of *trans*-cleavage for Smα1 variants: Smα1-L1 (square) and Smα1-L1 Δ1a (triangle); and for Pst3 variant Pst3-L1 (circle). Figure annotations are described in Fig. 1. Kinetic parameters are summarized in Table 1.

The *trans*-cleaving variant CChMVd-L1 (k_{obs} = 0.29 min^{-1}), which has loop I derived from CChMVd(+) (Fig. 2B), also showed a substantially improved cleavage rate when compared to the minimal derivative, CChMVd-min (k_{obs} < 0.01 min^{-1}). Variant CChMVd-L1* CU, with a CUCUCUC loop I sequence, showed markedly reduced cleavage efficiency (k_{obs} = 0.04 min^{-1}). The reaction for CChMVd-L1 was bi-phasic.

3.3. Deriving trans-cleaving hammerhead ribozyme variants from Smα1 and Pst3

Some natural hammerhead ribozyme species extend their sequences from helix I and terminate helices II and III with loops II and III, respectively [17]. We created *trans*-cleaving variants of Smα1 and Pst3 (from *Dolichopoda*), preserving the natural bulge (B1) found in each while extending helix I further before terminating with a stable GAAA tetraloop (Fig. 3A and B). Variant Smα1-L1, which has the natural bulge of Smα1, proved to be kinetically well-behaved, with a k_{obs} of 0.14 min^{-1} and 88% yield after 40 min at 10 mM $MgCl_2$. The minimal variant of Smα1-L1, which is known to be catalytically inefficient [11,12], was not used in this study. A direct comparison between Smα1-L1 and the standard minimal ribozyme sTRSV-min showed that the cleavage rate for Smα1-L1 was marginally better under the same conditions (k_{obs} of 0.14 min^{-1} for Smα1-L1 versus 0.10 min^{-1} for sTRSV-min, Table 1). Initially, it seemed that helix 1a may make Smα-L1 inflexible, thus impeding fast cleavage. However, Smα-L1 Δ1a, which lacks the hybridizing arm 1a (Fig. 3A), was much less effective than Smα-L1. Variant Pst3-L1 was catalytically ineffective.

4. Discussion

Here, we show that tertiary interactions between internal loops found in diverse natural *cis*-cleaving hammerhead ribozymes can be successfully recapitulated in a *trans*-cleaving ribozyme format for faster cleavage under single-turnover conditions. Yet, with the exception of PLMVd-L1, cleavage rates showed at most only a 4-fold improvement relative to the minimal derivative of sTRSV(+). Moreover, most variants with improved cleavage displayed a lower extent of cleavage (plateau), which suggests the presence of one or more inactive ribozyme conformations. Although enhanced *trans*-cleavage was obtained by simple transposition of natural loop I motifs, this alone is not sufficient to achieve optimal *trans*-cleavage, since these modifications have not been selected by biological evolution. Burke and colleagues [20] recently used SELEX to identify fast *trans*-ribozymes based on the PLMVd structure. Selected ribozymes, which cleaved exogenous targets containing a 5′ GUC 3′ triplet, showed enhanced activity at submillimolar levels of Mg^{2+} and thermal stability at higher reaction temperatures. Interestingly, these selected variants differed from the consensus PLMVd loop II sequence 5′ UGAR-AU 3′ by only a single nucleotide (underlined) [20]. This is in agreement with our data for the *trans*-cleaving variant PLMVd-L1, which cleaved with the highest initial rate and extent of cleavage when compared to the other *trans*-cleaving ribozymes tested and implies that tertiary interactions between internal loops of PLMVd-L1 are likely to be already close to optimal.

In our case, a correlation exists between the size of the natural loop I sequence and the corresponding catalytic efficiency of the modified *trans*-cleaving ribozyme. For PLMVd-L1, the tri-nucleotide sequence introduced into the hybridizing arm of helix I may allow for more efficient tertiary interactions than the seven-nucleotide loop I sequences of sTRSV-L1 and CChMVd-L1. Similarly, the extension of helices 1b and 1c along with the bulge sequences may make the structure of Smα1-L1 and Pst3-L1 unwieldy, preventing optimized tertiary interactions and perhaps even inducing catalytically inactive conformers. In particular, the very large asymmetrical bulge of Pst3-L1 may prove structurally unstable in this *trans*-cleaving context. Nevertheless, the secondary structure of Smα1-L1 allows for both helical arms to theoretically co-align and preserve the natural association of loop II and the internal bulge in helix I. SELEX could be used to identify fast-cleaving variants of Smα1-L1, where nucleotides within loop II and the internal bulge are randomized, allowing for catalytically less constrained tertiary associations than modified ribozymes based on PLMVd.

Modified *trans*-acting ribozymes cleave at physiologically relevant Mg^{2+} levels (0.1–1 mM) [21] as opposed to minimal *trans*-cleaving ribozymes which require >5 mM Mg^{2+} for effective cleavage. These data bode well for the use of modified *trans*-ribozymes in vivo, where more effective cleavage remains an important future objective.

Acknowledgments: We thank Mohammed Amarzguioui, Marjorie Robbins, Daniela Castanotto and Harris Soifer for critical reading and for helpful discussions. This work was supported by NIH grants AI29329 and AI42552 to J.J.R. M.S.W holds a James Gear Fellowship from the Poliomyelitis Research Foundation, South Africa.

References

[1] Forster, A.C. and Symons, R.H. (1987) Self-cleavage of plus and minus RNAs of a virusoid and a structural model for the active sites. Cell 49, 211–220.
[2] Hutchins, C.J., Rathjen, P.D., Forster, A.C. and Symons, R.H. (1986) Self-cleavage of plus and minus RNA transcripts of avocado sunblotch viroid. Nucleic Acids Res. 14, 3627–3640.
[3] Epstein, L.M. and Coats, S.R. (1991) Tissue-specific permutations of self-cleaving newt satellite-2 transcripts. Gene 107, 213–218.
[4] Rojas, A.A., Vazquez-Tello, A., Ferbeyre, G., Venanzetti, F., Bachmann, L., Paquin, B., Sbordoni, V. and Cedergren, R. (2000) Hammerhead-mediated processing of satellite pDo500 family transcripts from *Dolichopoda* cave crickets. Nucleic Acids Res. 28, 4037–4043.
[5] Ferbeyre, G., Smith, J.M. and Cedergren, R. (1998) Schistosome satellite DNA encodes active hammerhead ribozymes. Mol. Cell Biol. 18, 3880–3888.
[6] Hertel, K.J., Herschlag, D. and Uhlenbeck, O.C. (1994) A kinetic and thermodynamic framework for the hammerhead ribozyme reaction. Biochemistry 33, 3374–3385.
[7] Uhlenbeck, O.C. (2003) Less isn't always more. RNA 9, 1415–1417.
[8] Khvorova, A., Lescoute, A., Westhof, E. and Jayasena, S.D. (2003) Sequence elements outside the hammerhead ribozyme catalytic core enable intracellular activity. Nat. Struct. Biol. 10, 708–712.
[9] De la Peña, M., Gago, S. and Flores, R. (2003) Peripheral regions of natural hammerhead ribozymes greatly increase their self-cleavage activity. EMBO J. 22, 5561–5570.
[10] Yen, L., Svendsen, J., Lee, J.S., Gray, J.T., Magnier, M., Baba, T., D'Amato, R.J. and Mulligan, R.C. (2004) Exogenous control of mammalian gene expression through modulation of RNA self-cleavage. Nature 431, 471–476.

[11] Penedo, J.C., Wilson, T.J., Jayasena, S.D., Khvorova, A. and Lilley, D.M. (2004) Folding of the natural hammerhead ribozyme is enhanced by interaction of auxiliary elements. RNA 10, 880–888.
[12] Canny, M.D., Jucker, F.M., Kellogg, E., Khvorova, A., Jayasena, S.D. and Pardi, A. (2004) Fast cleavage kinetics of a natural hammerhead ribozyme. J. Am. Chem. Soc. 126, 10848–10849.
[13] Rueda, D., Wick, K., McDowell, S.E. and Walter, N.G. (2003) Diffusely bound Mg^{2+} ions slightly reorient stems I and II of the hammerhead ribozyme to increase the probability of formation of the catalytic core. Biochemistry 42, 9924–9936.
[14] Shimayama, T., Nishikawa, S. and Taira, K. (1995) Generality of the NUX rule: kinetic analysis of the results of systematic mutations in the trinucleotide at the cleavage site of hammerhead ribozymes. Biochemistry 34, 3649–3654.
[15] Stage-Zimmermann, T.K. and Uhlenbeck, O.C. (1998) Hammerhead ribozyme kinetics. RNA 4, 875–889.
[16] Sambrook, J., Fritsch, E.F. and Maniatis, T. (1989) Molecular Cloning: A Laboratory Manual, Cold Spring Harbor Laboratory Press, Cold Spring Harbor, NY, USA.
[17] Flores, R., Hernandez, C., de la Peña, M., Vera, A. and Daros, J.A. (2001) Hammerhead ribozyme structure and function in plant RNA replication. Methods Enzymol. 341, 540–552.
[18] Hernandez, C. and Flores, R. (1992) Plus and minus RNAs of peach latent mosaic viroid self-cleave in vitro via hammerhead structures. Proc. Natl. Acad. Sci. USA 89, 3711–3715.
[19] Navarro, B. and Flores, R. (1997) Chrysanthemum chlorotic mottle viroid: unusual structural properties of a subgroup of self-cleaving viroids with hammerhead ribozymes. Proc. Natl. Acad. Sci. USA. 94, 11262–11267.
[20] Saksmerprome, V., Roychowdhury-Saha, M., Jayasena, S., Khvorova, A. and Burke, D.H. (2004) Artificial tertiary motifs stabilize trans-cleaving hammerhead ribozymes under conditions of submillimolar divalent ions and high temperatures. RNA 10, 1916–1924.
[21] London, R.E. (1991) Methods for measurement of intracellular magnesium: NMR and fluorescence. Annu. Rev. Physiol. 53, 241–258.
[22] Leontis, N.B. and Westhof, E. (2001) Geometric nomenclature and classification of RNA base pairs. RNA 7, 499–512.